Specialty fibers for sensors and sensor components

R. Yamauchi, K. Himeno, T. Tsumanuma, and R. Dahlgren*

Fujikura, Ltd., Optoelectronics Laboratory
1440 Mutsuzaki, Sakura, Chiba, 285 Japan

*Fujikura Technology America Corp.
3001 Oakmead Village Drive, Santa Clara, CA 95051

ABSTRACT

This paper surveys a variety of special fibers which have been developed for the sensor and component markets, based upon the Polarization-maintaining And Absorption-reducing (PANDA) design. Various types of polarization-maintaining (PM) fibers, rare-earth doped fibers, image-transmitting fibers, and other special fibers will be discussed.

1. INTRODUCTION

PANDA polarization-maintaining fibers [1] have been developed over a period of years by NTT and Fujikura into a variety of specialized optical fibers for sensor applications. Interferometric fiber optic sensors often demand preservation of a linear state-of-polarization (SOP), and other sensors require deterministic retardation values in the fiber. This paper will review fibers used in these applications, and special fibers developed for the fabrication of sensor building blocks such as PM couplers, amplifiers, polarizers, and splices.

2. POLARIZATION-MAINTAINING FIBER

2.1 High performance PANDA fiber

The cross-section of a typical PANDA fiber is shown in Figure 1A, which consists of a pure silica cladding and a Germanium-doped core region. The Ge-doping tends to increase the refractive index of the core region, which is designed to guide the two lowest-order eigenmodes. A pair of Stress Applying Parts (SAPs), which are made from a borosilicate glass, are located on either side of the core. The SAPs have a greater thermal coefficient of expansion than does the surrounding cladding. This structure will induce stress, and therefore linear birefringence, as the fiber cools during the drawing process; the two lowest-order eigenmodes will no longer be degenerate and will propagate at different velocities. A set of principal axes can now be defined, and are often denoted the slow and fast principal axes of the optical fiber. If the birefringence $\Delta\beta$ can be made large compared to externally-induced (and random) birefringence perturbations, a linear SOP launched into one of the principal axes will be preserved [2].

PANDA fiber has been made for numerous wavelengths with losses as low as 0.22 dB/km at 1.55 μm wavelength [1]. Table 1 summarizes some of the parameters of PANDA fibers available for sensor applications. For more details of PANDA fiber, refer to [1-3], and references cited therein.

2.2 Bend resistant PANDA fiber

One major application for PM fiber is in the Fiber Optic Gyroscope (FOG); this and other sensor configurations require small-diameter coiling of the fiber to minimize sensor size. Often there is an additional requirement of small cladding and coating diameters to help reduce the sensing coil volume. By utilizing smaller core diameter and a larger amount of Ge-doping than for standard PANDA fiber several things happen: the Δn between core and cladding increases, the modes are more tightly guided, and the numerical aperture (NA) increases. If high-birefringence can be maintained along with these conditions, improved attenuation and polarization performance under bending conditions will result [2-5]. By careful tradeoff of these factors, and proper coating design, acceptable performance can be achieved over a wide temperature range (See Figure 2).

Table 1. PANDA fiber performance.

fiber type	λ μm	loss dB/km	min bend dia mm	biref $\times 10^{-4}$	crosstalk dB 1km	M.F.D. μm
Normal	0.85	2.0	20	7.0	-20	5.5
	1.3	0.5	30	4.5	-20	9.0
	1.55	0.3	40	4.5	-20	10.5
High NA	0.85	2.8	10	7.0	-25	3.5
	1.3	1.0	15	6.5	-25	5.5
	1.55	1.0	20	6.5	-25	6.5
D.S.F.	1.55	0.35	40	3.0	-20	8.0
Pure-Silica	1.55	0.2	50	4.0	-20	10.5
Coupler	0.82	-	20	2.5	-10	5.0
Single-Pol.	0.85	2.7	80	8.6	47 (ER)	-

2.3 Dispersion-shifted PANDA fiber

A new type of PANDA fiber has been recently developed, which is a dispersion-shifted design, as shown in Figure 1B. Most fibers have zero dispersion near 1.3 μm wavelength, but a more complex core region can make a PM dispersion-shifted fiber (DSF) possible, having a zero-dispersion wavelength region of 1.52 ~ 1.58 μm, with a dispersion value less than ± 3 ps/km over that wavelength range.

2.4 Radiation resistant PANDA fiber

A pure-silica core version of PANDA fiber has been fabricated for high-radiation environments. The structure for this fiber is shown in Figure 1C, having an undoped core, and depressed-index Fluorine-doped cladding. Steady-state testing of 1.3 μm PM fibers using a Co^{60} source at a dose rate of 50 rads/sec has been reported by the Naval Research Lab [6]. The short-term and longer-term behavior is shown in Figure 3A and 3B for Fujikura radiation-hardened (RH) fiber. In that study, the RH fiber exhibited a larger initial loss, which tended to saturate at a lower level compared to other fibers. Figure 3C illustrates the recovery after 10 Krads total dose; note the Fujikura RH fiber recovers quickly to a low loss value, and the Ge-doped PANDA fiber also performs well.

2.5 Single-polarization PANDA fiber

By careful design of PANDA fiber, one of the two eigenmodes can be made relatively lossy compared to the other. In this case, the fiber behaves as a distributed polarizer, and will attenuate one eigenmode, and transmit the orthogonal SOP with low attenuation [7]. The attenuation values for the eigenmodes are strong functions of wavelength and coil diameter, which must be considered in the use of these fibers. This fiber has been useful in the development of fiber optic polarizers and single-polarization resonators for FOG applications [8].

2.6 Splicing characteristics

To permanently connect PM optical fibers and PM components, special fusion splicing schemes have been developed for PANDA fiber. The Profile Alignment System (PAS) observes the SAP structure to identify and align the fast and slow axes of the PM fiber [9]. In this manner, it is not necessary to actively launch light into the fiber core and align the fiber's principal axes manually. PAS splicing will obtain polarization crosstalk values averaging -32 dB for PANDA fiber.

2.7 Couplers and Matched-index PANDA fiber

Researchers have reported high-performance polished [10, 11], fused [12, 13], and polished/fused couplers [14] made from PANDA fiber, and several commercial sources are available [15]. High-quality 2×2 PM couplers have losses < 0.5 dB and polarization cross-coupling in the 20 ~ 30 dB range.

There is increased difficulty in fabricating high-performance fused PM couplers with standard PANDA fiber, because the SAPs have a slightly depressed index as shown in Figure 1A. By adding germanium to the borosilicate SAP material, the SAP refractive index can be compensated to nearly match the cladding, as shown in Figure 1D. This type of PANDA fiber design permits low-loss couplers to be fabricated which are stable over a wide temperature range. The stability of fused couplers made from different types of fiber is compared in Figure 4A and 4B after a number of temperature cycles [12]. The devices reported in that study operate at 0.8 μm wavelength, and are packaged in a 32-mm long, 2.5-mm diameter stainless steel tube.

3. ERBIUM-DOPED FIBER

3.1 Erbium-doped single-mode fiber

A high NA erbium-doped single-mode fiber was manufactured, employing Ge-doping in the core and F-doping in the cladding to get an overall $\Delta = 1.6\%$. A small-diameter core further concentrates the pump and signal and the Er-doping and Al-codoping are also in the core region. The interested reader is referred to [16], which discusses design and fabrication of a high NA Erbium fiber, Erbium-doped DSF, and radiation effects on Erbium-doped fibers.

When assembling amplifiers using fusion splicing, modal matching of normal fiber to high NA Erbium-doped fiber is important to avoid a 3~5 dB reduction of amplifier gain [17]. Mode matching is accomplished after splicing, by diffusion of the core dopants in the splice region at a high temperature. An optical amplifier has been constructed in the forward-pumping configuration, using a 1.48 μm pump laser. At the signal wavelength of 1.552 μm, power conversion of up to 75% was demonstrated at 50 mW pump power.

3.2 Erbium-doped twin-peak core (TPC) fiber

A type of PM rare-earth doped fiber which has been demonstrated consists of two closely-spaced cores, as shown in Figure 1E, with $\Delta = 1.48\%$. The two cores produces a shape birefringence of approximately 1.6×10^{-4} at $\lambda = 1.55$ μm, low polarization crosstalk, and good splicability to standard PM fibers [18]. For 57 m of fiber at a signal power of -40 dBm, and the same conditions as above, the gain efficiency was about 2.2 dB/mW of pump power. This is compared to 2.1 dB/mW for 26 m of single-mode Erbium-doped fiber under the same conditions.

3.3 Erbium-doped PANDA fiber

Recently, an Erbium-doped PANDA fiber has been demonstrated [3], which has high birefringence of roughly 5×10^{-4} at 1.55 μm. This fiber is illustrated in Figure 1F. The small-signal and saturated gain for this fiber are shown in Figures 5A and 5B, respectively. This fiber is finding applications in experiments such as modelocked ring lasers for the generation of stable picosecond pulses [19, 20].

4. IMAGE BUNDLE FIBER

4.1 High-resolution imagefiber

High resolution imaging bundles have been fabricated for the medical industry, with resolutions of 6000 pixels in a 0.5 mm diameter; up to 100,000 pixels are possible on larger bundles. The individual cores of the bundle are sufficiently small to be single-mode at visible wavelengths [21]. This type of imagefiber exhibits a transmission that is a strong function of wavelength, and visible-light images would be highly tinted. However, for some applications which use monochromatic light, it is highly desirable to have single-mode imagefiber [21, 22]. Figure 6 plots the spectral attenuation for a typical germanium-doped imagefiber bundle.

4.2 Radiation resistant imagefiber

By using a similar design to the radiation-hard fiber described in §2.4, imagefiber can be fabricated with pure-silica core and a depressed-index cladding [23]. This type of imagefiber has excellent resistance to radiation,

exhibiting roughly 0.15 dB/m loss increase for a total dose of 1 Mrad, as shown by Figure 7. The data was taken at 250°C temperature at a steady-state dose rate of 5 Krads/hr. This fiber has found use nuclear industrial inspection systems, and inspection applications where survival at high temperatures is required.

5. ULTRAVIOLET TRANSMITTING FIBER

Figure 8 describes the characteristics of a newly developed UV-transmitting fiber, which may be configured as a multimode fiber or a nonimaging (incoherent) bundle. Figure 8A is the attenuation spectrum for a multimode UV-transmitting fiber, showing a loss of about 0.3 dB/m at 248 nm. Figure 8B shows the increase of attenuation at 248 nm after repeated exposure to 248 nm KrF laser 0.5 mJ/mm^2 pulses at a rep rate of 200 Hz. This fiber is showing potential for new surgical techniques within the human body using excimer lasers.

6. CONCLUSIONS

In summary, a number of special fibers have been developed for sensor applications at Fujikura. Of particular interest are high NA fibers for compact sensing coils, and matched-SAP-index fiber for fused PM coupler manufacture. Other special PANDA fiber designs which have been developed are dispersion-shifted, radiation-hardened, and single-polarization types. These fibers are finding applications in niche markets worldwide.

Erbium-doped silica fiber has revolutionized the long-haul telecom industry, by making all-fiber optical amplifiers possible at the 1.55 μm wavelength region. High NA, PANDA, and twin-core variants have been demonstrated for sensor R&D projects.

Bundle-fiber technology has been refined to produce ultrahigh-resolution, radiation-hardened, and UV-transmitting fiber products. These have many emerging applications in industrial inspection and medical applications.

7. ACKNOWLEDGMENTS

8. REFERENCES

1. Y. Sasaki, T. Hosaka, M. Horiguchi, and J. Noda, "Design and fabrication of low-loss and low-crosstalk polarization-maintaining optical fibers," *IEEE Journal of Lightwave Technology*, Vol. 4, No. 8, pg. 1097-1102 (1986).

2. K. Inada, "Special Optical Fibers for Sensors," *International Conference on Optical Fibre Sensors in China*, SPIE Vol. 1572, pg. 163-168 (Bejing, 1991).

3. K. Himeno, *et al.*, "Polarization-maintaining optical fibers," *Fujikura Giho (in Japanese)*, No. 85, pg. 1-9 (1993).

4. Y. Kikuchi, K. Himeno, O. Fukuda, and K. Inada, "High birefringence fiber with high numerical aperture for compact optical components," *Sino-Japanese OFSET'87*, pg. 149-154 (1987).

5. Y. Kikuchi, N. Kawakami, K. Himeno, O. Fukuda, and K. Inada, "Crosstalk in polarization maintaining optical fiber," *OEC'88*, Vol. 4B2-3, pg. 126-127 (1988).

6. E.J. Friebele, *et al.*, "Radiation effects in polarization-maintaining fibers," *Fibre Optics'90*, SPIE Vol. 1314, pg. 146-154 (1990).

7.   K. Himeno, Y. Kikuchi, N. Kawakami, O. Fukuda, and K. Inada, "A high-extinction-ratio and low-loss single-mode single-polarization optical fiber," *OFS'88*, OSA pg. 472-475 (New Orleans, 1988).

8.   R.P. Dahlgren and R.E. Sutherland, "Single-polarization fiber-optic resonator for gyro applications," *Fiber Optic Gyros: 15th Anniversary Conference*, Proc. SPIE Vol. 1585, pg. 128-135 (Boston, 1991).

9.   H. Taya, K. Ito, T. Yamada, and M. Yoshinuma, "New splicing method for polarization-maintaining fibers," *OFC'89*, Optical Society of America pg. 164-165 (Houston, 1989).

10.   T. Arikawa, F. Suzuki, Y. Kikuchi, O. Fukuda, and K. Inada, "Ultra-low-crosstalk polarization maintaining optical fiber coupler," *Optical Fiber Sensors*, OSA Vol. 2, pg. 480-483 (New Orleans, 1988).

11.   R.P. Dahlgren, "Studies in Fiber-Optic Couplers and Resonators," Massachusetts Institute of Technology S.M. Thesis (1993).

12.   Y. Anjan and S. Habbel, "Environmental Performance of fused PM fiber couplers for fiber gyro application," *IEEE Photonics Technology Letters*, Vol. 3, No. 6, pg. 578-580 (1991).

13.   E. Fiumara, A. Durante, G. Saffioti, and G. Serra, "Reproducable, unfriendly environment resistant, optical fiber polarization-maintaining fused couplers," *Optoelectronic Devices and Applications*, SPIE Vol. 1338, pg. 11-17 (1990).

14.   C.V. Cryan, M.O. Donnchadha, J.M. Lonergan, and C.D. Hussey, "Fused polished polarization-maintaining fibre couplers," *Electronics Letters*, Vol. 28, No. 9, pg. 857-858 (1992).

15.   Alcoa-Fujikura Ltd., Gould Fiber Optics Inc., Canadian Instruments & Research Ltd., Japan Avation Electronics Industry Ltd.

16.   A. Wada, D. Tanaka, T. Sakai, and R. Yamauchi, "Er-doped optical fiber amplifiers for 1.55μm transmission," *Fujikura Technology Review*, Vol. 20, pg. 1-10 (1991).

17.   A. Wada, *et al.*, "1.55μm high efficiency Er-doped optical fiber amplifiers," *Fujikura Technology Review*, Vol. 20, pg. 11-16 (1991).

18.   K. Himeno, *et al.*, "New polarization-maintaining amplifier using an Er-doped twin-peak core fiber," *OFC'94*, OSA pg. 278-279 (San Jose, 1994).

19.   H. Takara, S. Kawanishi, M. Saruwatari, and K. Noguchi, "Generation of highly stable 20 GHz transform-limited optical pulses from actively modelocked Er-doped fiber lasers with an all-polarization maintaining ring cavity," *Electronics Letters*, Vol. 28, No. 22, pg. 2095-2096 (1992).

20.   H. Takara, S. Kawanishi, and M. Saruwatari, "20 GHz transform-limited optical pulse generation and bit-error-free operation using a tunable, actively modelocked Er-doped fiber ring laser," *Electronics Letters*, Vol. 29, No. 13, pg. 1149-1150 (1993).

21.   L.S. Kiat, K. Tanaka, T. Tsumanuma, and K. Sanada, "Ultrathin single-mode imagefiber for medical usage," *Optical fibers in medicine*, SPIE Vol. 1649, pg. 208-217 (1992).

22.   A.F. Gmitro and D. Aziz, "Confocal microscopy through a fiber-optic imaging bundle," *Optics Letters*, Vol. 18, No. 8, pg. 565-567 (1993).

23.   T. Tsumanuma, S. Chigira, and K. Sanada, "Picture image transmission-system by fiberscope," No. 15, pg. 1-10 (1986).
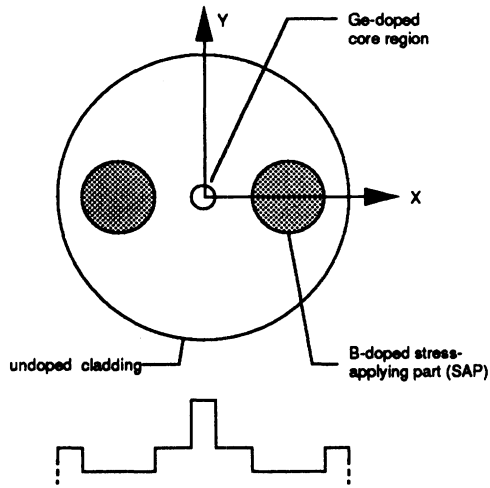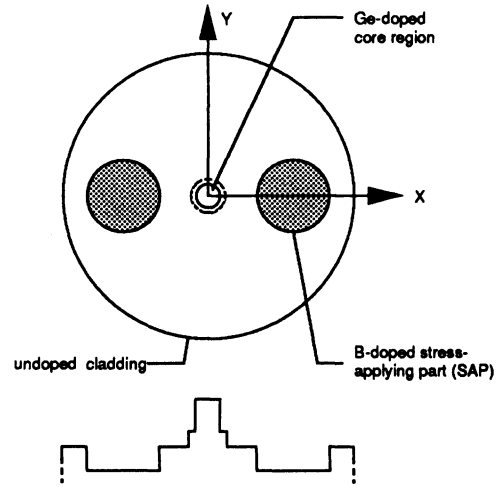
Y

Ge-doped
core region

X

undoped cladding

B-doped stress-
applying part (SAP)

Figure 1A. Standard PANDA fiber

Y

Ge-doped
core region

X

undoped cladding

B-doped stress-
applying part (SAP)

Figure 1B. Dispersion-shifted PANDA

Y

undoped
core region

X

F-doped cladding

B-doped stress-applying part (SAP)
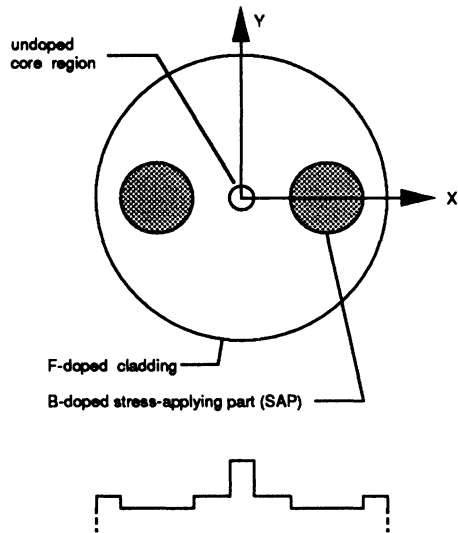
Figure 1C. Pure-silica core PANDA.

Y

Ge-doped
core region

X

undoped cladding

B-doped and Ge-doped SAP
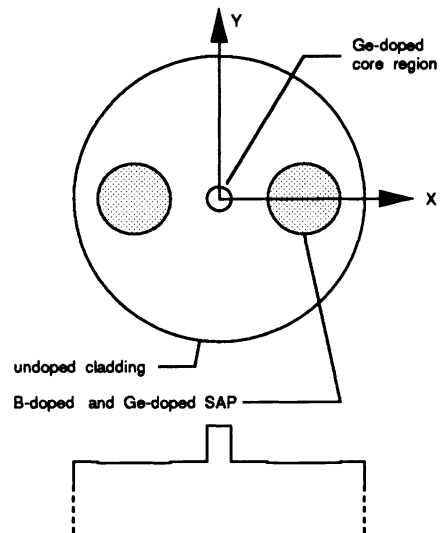
Figure 1D. PANDA fiber for coupler.

Y

Ge-doped
ER-doped
Al-doped
core regions

X

F-doped cladding
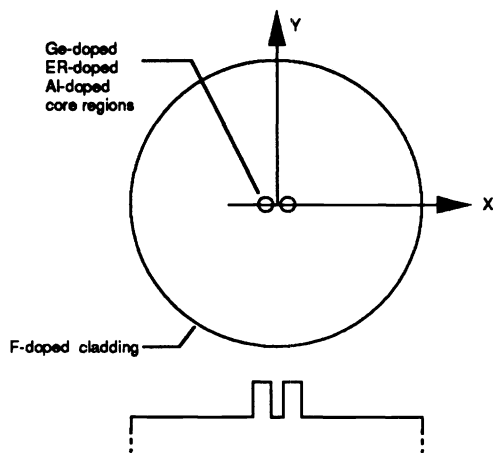
Figure 1E. Erbium-doped TPC fiber.

Y

Ge-doped
Er-doped
Al-doped
core region

X

undoped cladding

B-doped stress-applying part (SAP)
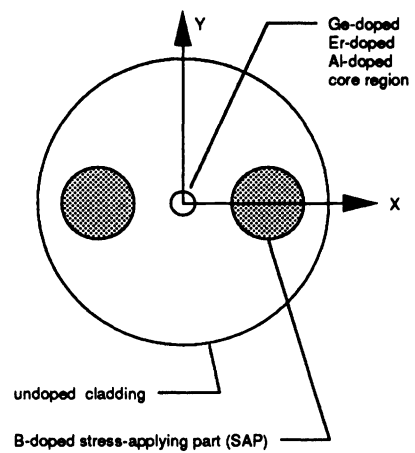
Figure 1F. Erbium-doped PANDA
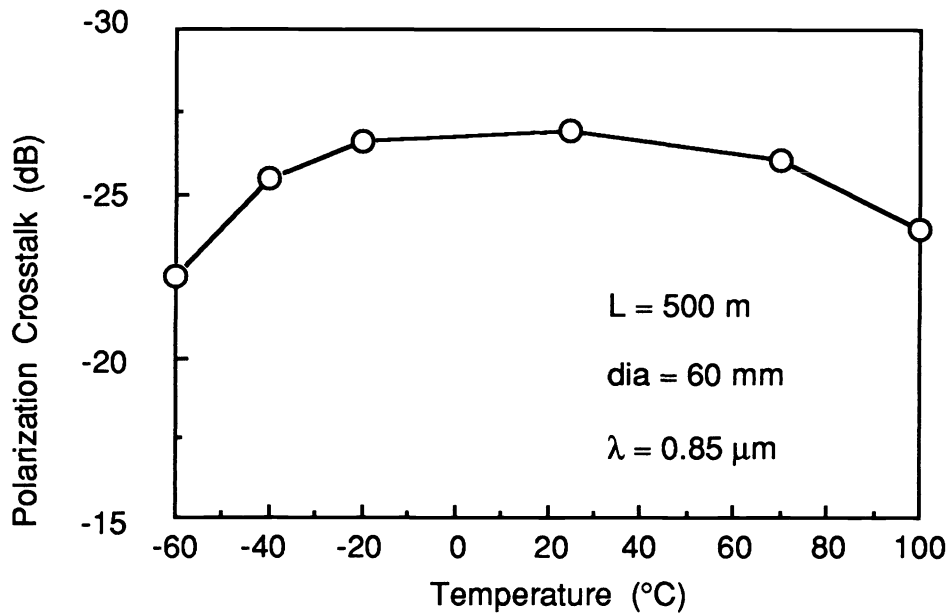
Figure 2. Polarization crosstalk as a function of
temperature for high-NA PANDA fiber
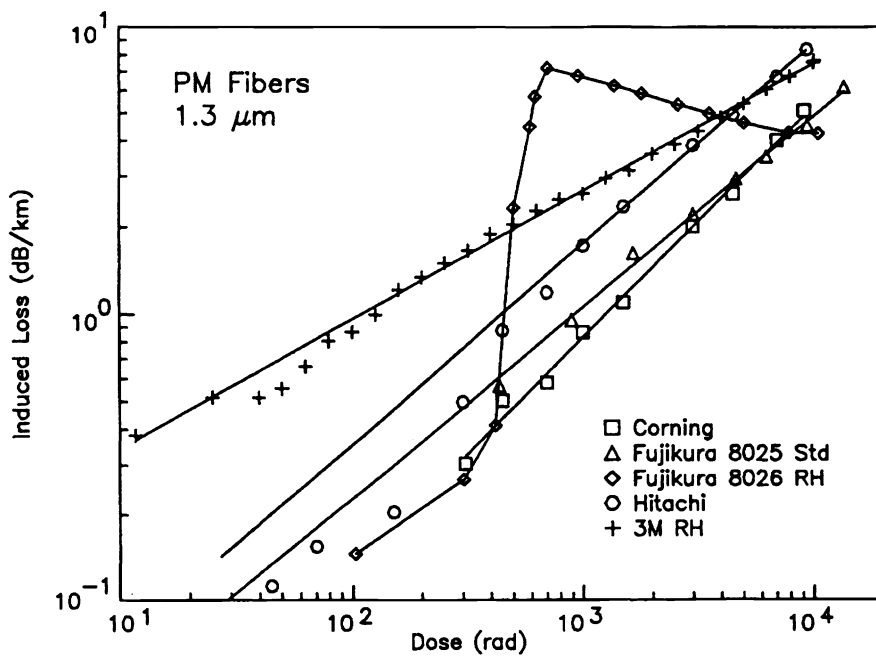
Figure 3A.   Differential attenuation induced in
PM fibers by steady-state irradiation [6].
(Reproduced with permission)
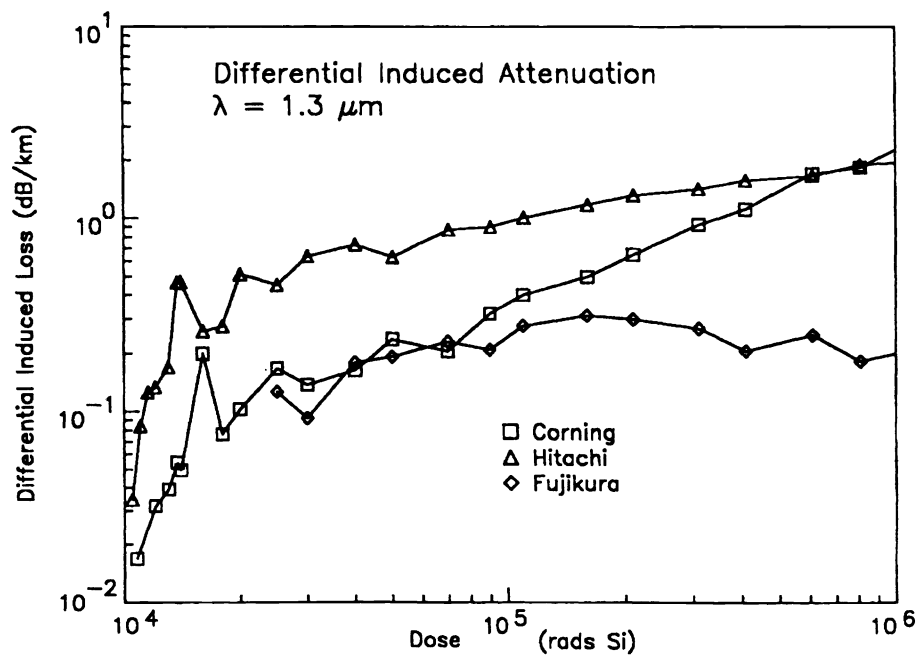
Figure 3B.   Differential attenuation induced in
PM fibers by steady-state irradiation [6].
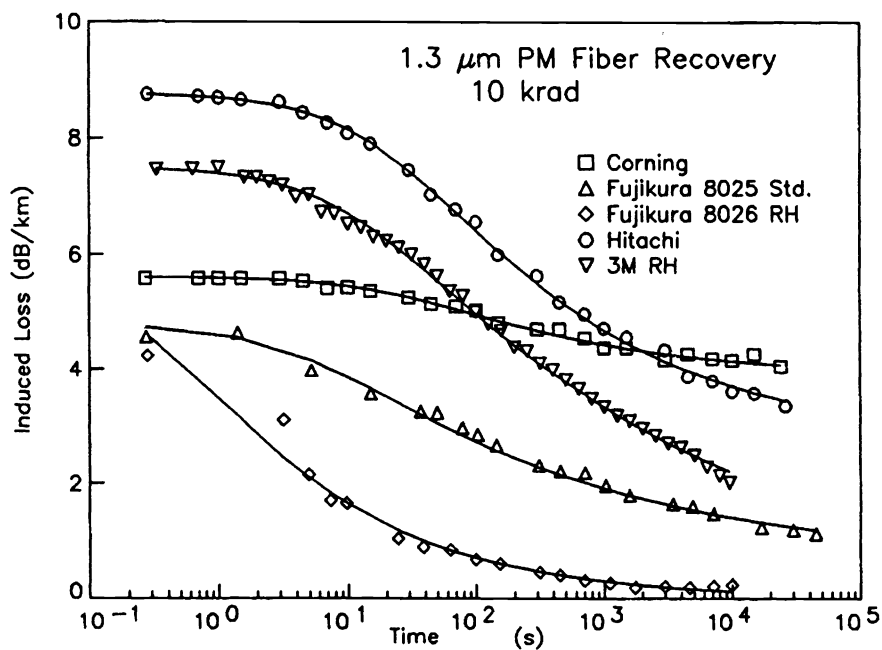
Figure 3C.   Recovery characteristics of PM fibers
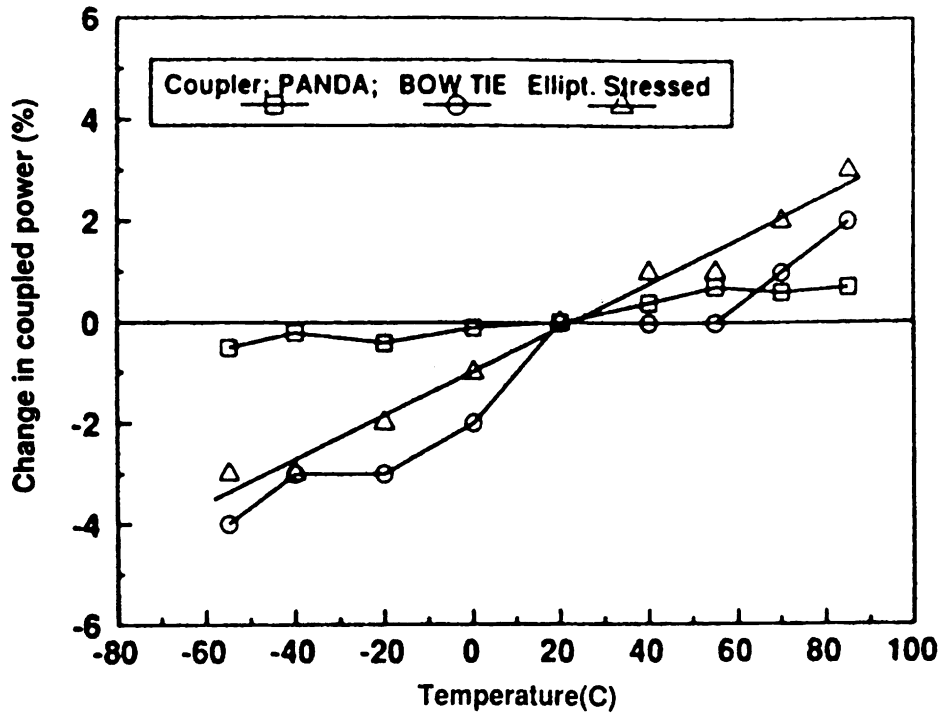following a high dose-rate exposure [6].

Figure 4A. Change in splitting ratio as a function
of temperature for fused couplers [12]. © 1991 IEEE
(Reproduced with permission)
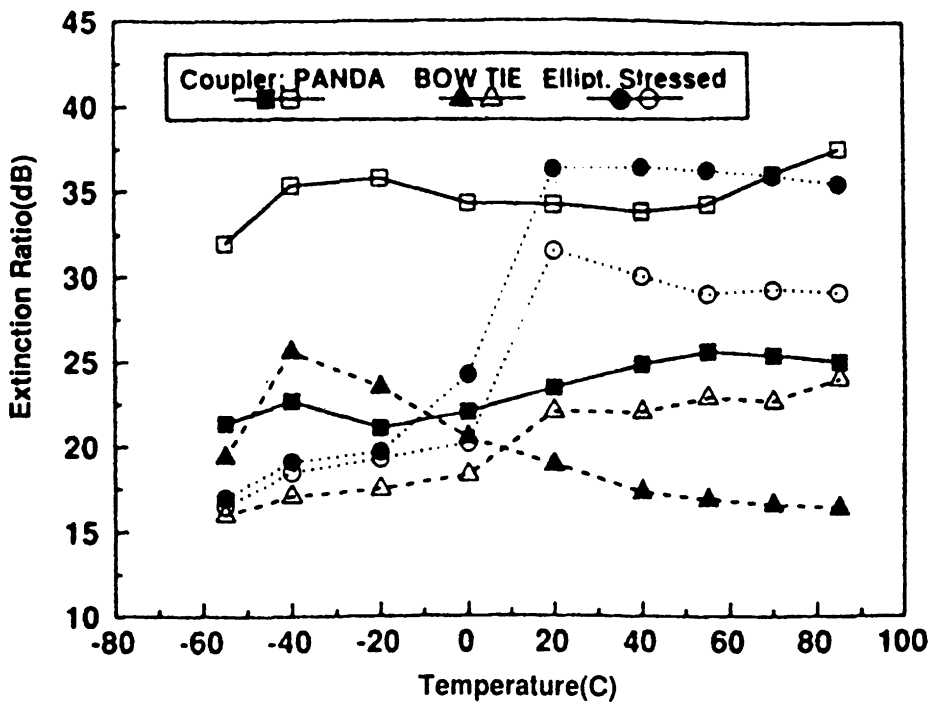
Figure 4B. Change in cross-coupling for throughput ■ and
coupled □ ports as a function of temperature [12]. © 1991 IEEE
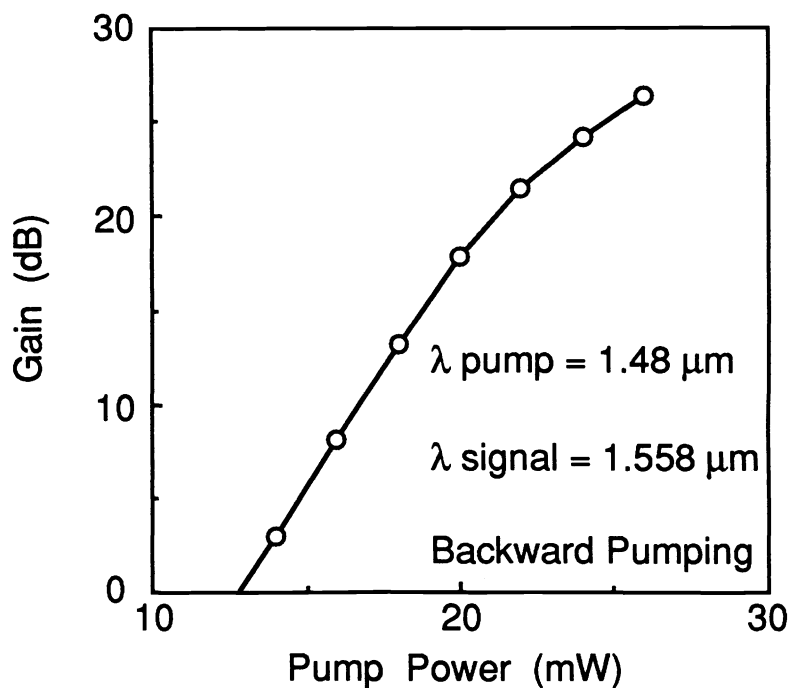
Figure 5A. Gain of Er-doped PANDA fiber in the small-
signal regime.   Signal power = -40 dBm
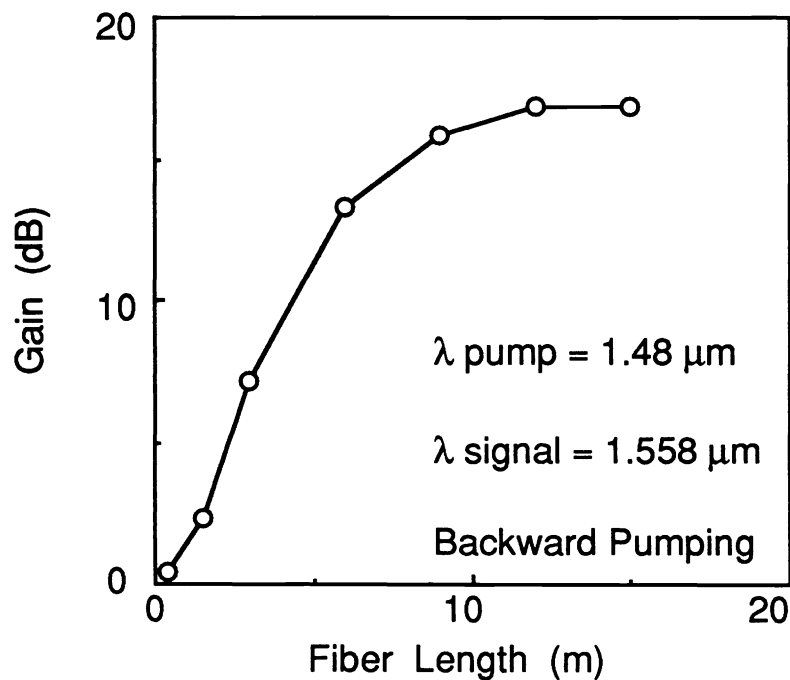
Figure 5B. Gain of Er-doped PANDA fiber in the saturated regime.
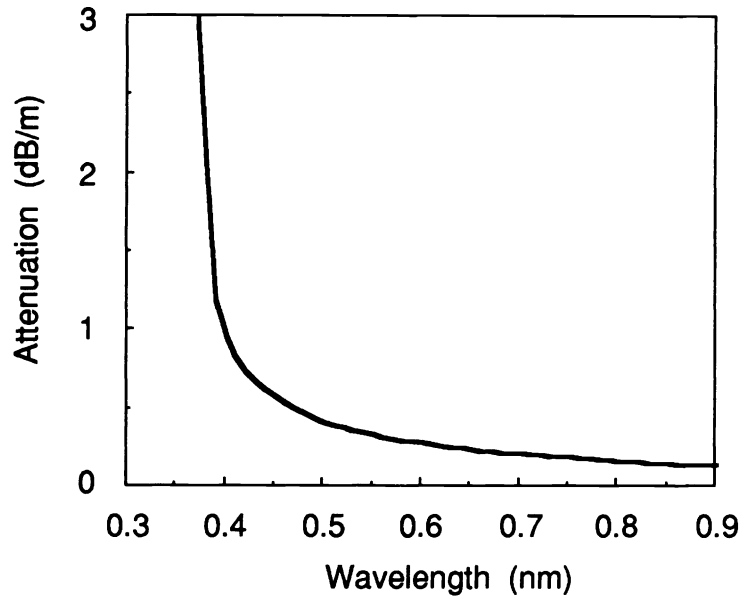Signal power = -0.5 dBm   Pump power = 90 mW

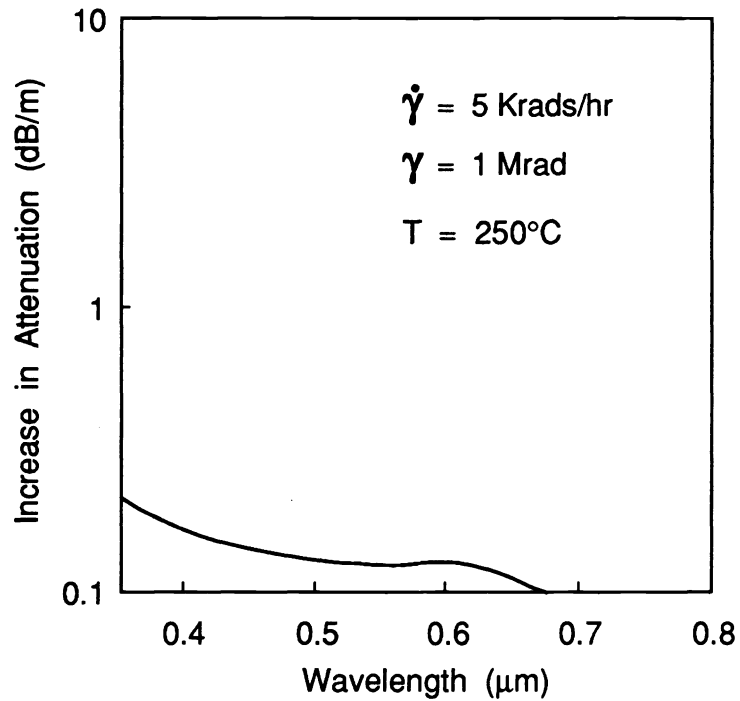Figure 6. Attenuation spectrum for high-resolution imagefiber.

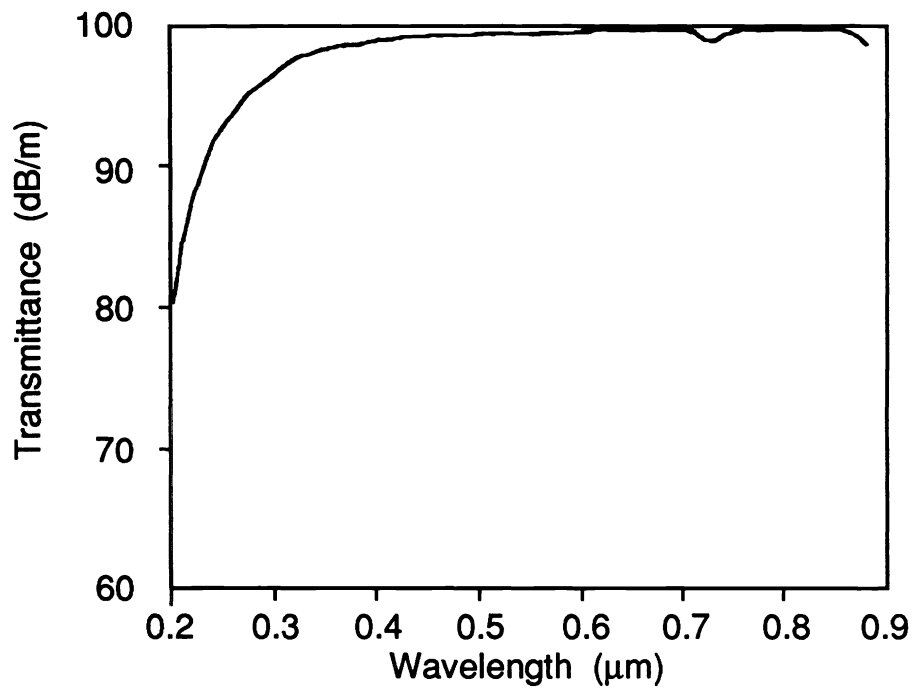Figure 7. Radiation effect on pure-silica imagefiber.

Figure 8A. Transmittance for UV-transmitting fiber.
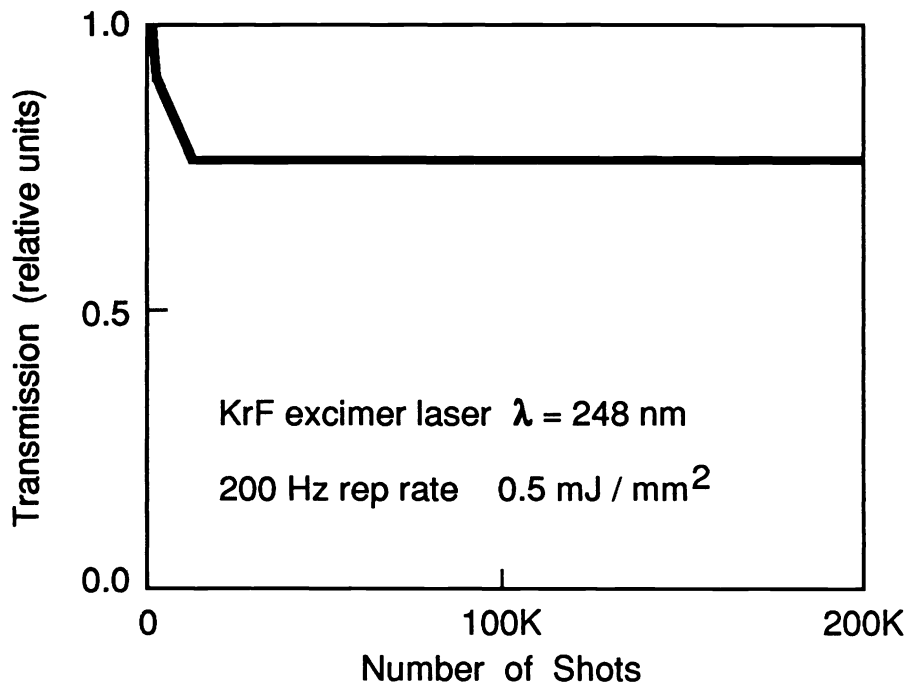

KrF excimer laser λ = 248 nm

200 Hz rep rate   0.5 mJ / mm^2

Figure 8B. UV-radiation effect on UV-transmitting fiber.